

# Making optical atomic clocks more stable with $10^{-16}$ -level laser stabilization

Y. Y. Jiang<sup>1,2</sup>, A. D. Ludlow<sup>1\*</sup>, N. D. Lemke<sup>1,3</sup>, R. W. Fox<sup>1</sup>, J. A. Sherman<sup>1</sup>, L.-S. Ma<sup>2</sup> and C. W. Oates<sup>1</sup>

**The superb precision of an atomic clock is derived from its stability. Atomic clocks based on optical (rather than microwave) frequencies are attractive because of their potential for high stability, which scales with operational frequency. Nevertheless, optical clocks have not yet realized this vast potential, due in large part to limitations of the laser used to excite the atomic resonance. To address this problem, we demonstrate a cavity-stabilized laser system with a reduced thermal noise floor, exhibiting a fractional frequency instability of  $2 \times 10^{-16}$ . We use this laser as a stable optical source in a ytterbium optical lattice clock to resolve an ultranarrow 1 Hz linewidth for the 518 THz clock transition. With the stable laser source and the signal-to-noise ratio afforded by the ytterbium optical clock, we dramatically reduce key stability limitations of the clock, and make measurements consistent with a clock instability of  $5 \times 10^{-16}/\sqrt{\tau}$ .**

In principle, the instability of an atomic clock at a certain averaging time is approximately given by the ratio of the transition linewidth to the transition frequency ( $\delta\nu/\nu_0$ ) divided by the measurement signal-to-noise ratio at that time. Optical atomic clocks based on large ensembles of atoms benefit not only from a large  $\nu_0$ , but also from a potentially large signal-to-noise ratio. This makes them strong candidates for achieving a measurement instability of  $\leq 1 \times 10^{-17}$  in 1 s. However, this stability remains far from realized. In a seminal research effort in 2001, two optical atomic clocks at the National Institute of Standards and Technology (NIST) were directly compared with a frequency comb<sup>1</sup>. The instability of these clocks was shown to be at record levels,  $\sim 4 \times 10^{-15}/\sqrt{\tau}$  (for measurement time  $\tau$ , in seconds). Research laboratories around the world have continued to refine optical atomic clocks since, reaching new levels of ultimate uncertainty, in the most extreme case  $\leq 1 \times 10^{-17}$  (ref. 2). However, the stability of these systems has not significantly improved, so characterizing these clocks at improved levels requires long averaging times. In fact, as microwave clocks (with  $\nu_0$  five orders of magnitude smaller) have reached their fundamental stability limit, they have achieved an instability<sup>3</sup> that is only ten times worse than that achieved by the best optical clocks so far. Similarly, large-ensemble optical clocks with promising signal-to-noise ratios have so far only demonstrated stability similar to those of optical clocks based on single ions. As a result, systems such as optical lattice clocks based on neutral ytterbium and strontium remain far from achieving their potential.

Clock stability is commonly limited by an imperfect clock laser, called here the local oscillator (LO). LO frequency noise limits coherent probing of the atom ensemble to times usually well below 1 s (limiting  $\delta\nu$ ). For times shorter than a measurement cycle, clock stability is determined entirely by the LO. At longer times, the clock stability is often limited by the Dick effect<sup>4,5</sup>:

because a measurement cycle includes atom preparation time, only a fraction of the cycle actually probes the atomic transition (that is, measures the LO frequency relative to the transition frequency). This periodic sampling of the LO aliases higher-frequency LO noise, limiting the clock stability that can be achieved. In neutral atom systems, the Dick limit is usually well above fundamental limits such as quantum projection noise<sup>6</sup> and often corresponds closely with the experimentally observed clock instability<sup>1,7-9</sup>. Improving LO stability directly reduces the Dick effect both by reducing the frequency noise that is aliased and by enabling longer atomic probe times, which reduces the fractional 'dead' time between consecutive probe cycles. Improved LO performance thus plays a critical role in realizing the high stability possible with many optical atomic clocks. Note also that because stable LOs offer narrower  $\delta\nu$ , other clock instability limits decrease<sup>6</sup>. As instability typically averages as  $1/\sqrt{\tau}$ , improving the stability at a given time greatly reduces the required averaging time, as the square of the improvement.

State-of-the-art laser stabilization usually involves phase-locking a laser source (with electronic feedback) to a single longitudinal and transverse mode of a passive, ultrastable Fabry-Pérot (FP) cavity (Fig. 1). The FP cavity consists of very high-reflectivity mirrors, optically contacted onto a rigid spacer. In the limit of good signal-to-noise ratio and tight phase lock, the length stability of the FP cavity gives the frequency stability of the resulting optical

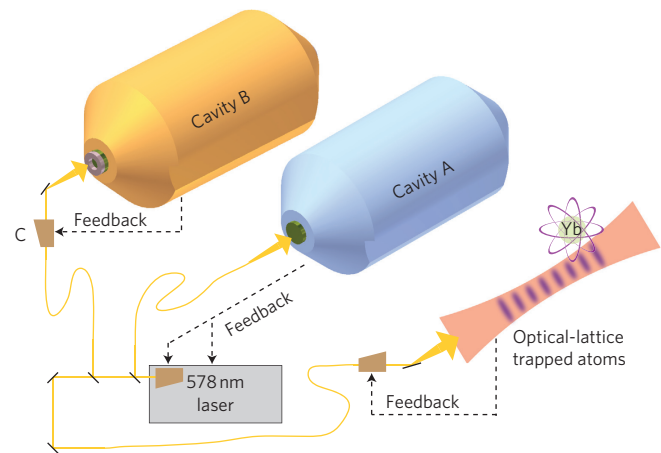


**Figure 1 | Experimental set-up.** Laser light at 578 nm is incident on two independent, isolated optical cavities. Each cavity is composed of a rigid ULE spacer with optically bonded fused-silica mirror substrates. Feedback for laser frequency control is usually applied to acousto-optic modulators. The stabilized light probes the narrow clock transition in an ultracold sample of ytterbium, confined in a one-dimensional optical lattice.

<sup>1</sup>National Institute of Standards and Technology, 325 Broadway, Boulder, Colorado 80305, USA, <sup>2</sup>State Key Laboratory of Precision Spectroscopy, East China Normal University, 3663 ZhongShan Road, Shanghai, China, <sup>3</sup>University of Colorado, Department of Physics, Boulder, Colorado 80309, USA.

\*e-mail: ludlow@boulder.nist.gov

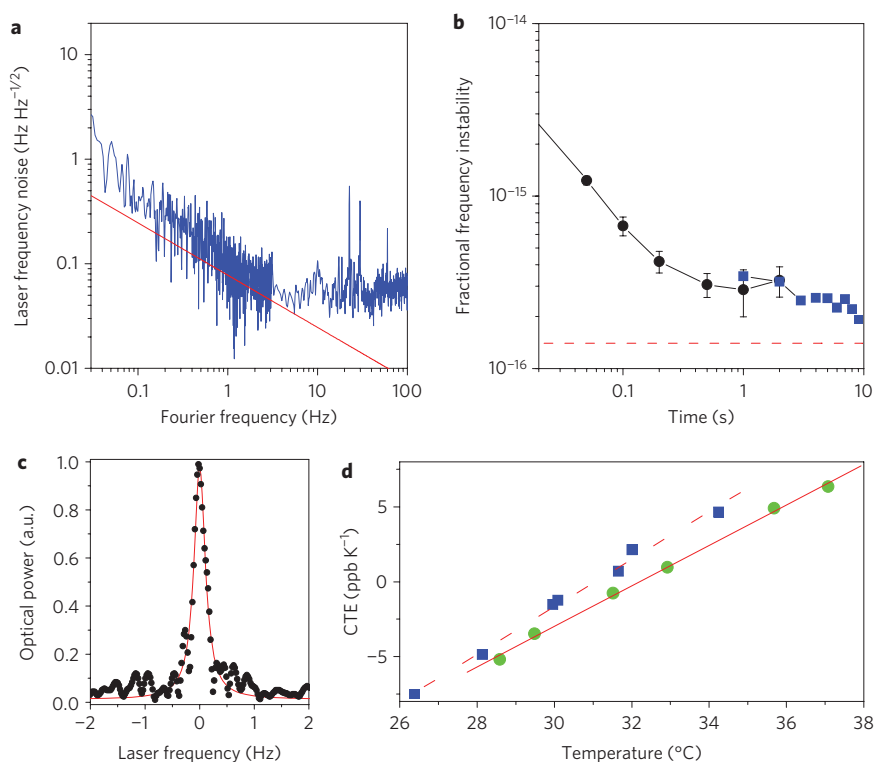


**Figure 2 | Stable laser properties.** **a**, Frequency noise spectrum (blue data) and theoretical estimate of the thermal noise (red line). **b**, Fractional frequency instability of one cavity. Blue squares derive from frequency counting with an Agilent 53132 counter<sup>28</sup> (1 s gate time, juxtaposed data set, with linear drift of  $\sim 250$  mHz s<sup>-1</sup> removed), and black circles are from an SRS 620 counter (using a built-in Allan deviation tool, one sigma error bars shown). The red dashed line denotes the Brownian thermal-noise-limited instability. **c**, Laser power spectrum (black dots) and Lorentzian fit (red trace) with FWHM linewidth of 250 mHz (resolution bandwidth, 85 mHz). **d**, Measured CTE<sub>cav</sub> versus temperature for Cavity A (green dots with solid linear fit) and Cavity B (blue squares with dashed linear fit).

wave. A fundamental limit that many cavity-stabilized lasers have reached is given by Brownian thermal mechanical fluctuations of the FP cavity. The fractional frequency instability limit from thermal noise is typically dominated by the two cavity mirrors<sup>10,11</sup>:

$$\sigma_{\text{therm}} = \sqrt{\ln 2 \frac{8k_{\text{B}} T 1 - \sigma^2}{\pi^{3/2} E w_0 L^2} \left( \phi_{\text{sub}} + \phi_{\text{coat}} \frac{2}{\sqrt{\pi}} \frac{1 - 2\sigma d}{1 - \sigma w_0} \right)} \quad (1)$$

Here,  $\sigma$ ,  $E$  and  $\phi_{\text{sub}}$  are Poisson's ratio, Young's modulus and the mechanical loss for the mirror substrate,  $w_0$  is the laser beam ( $1/e$  field) radius on the mirror,  $T$  is the mirror temperature (K),  $k_{\text{B}}$  is Boltzmann's constant and  $L$  is the cavity length.  $\phi_{\text{coat}}$  and  $d$  denote the mechanical loss and thickness of the thin-film reflective coating. The first term in parentheses is the mirror substrate contribution and the second term is the contribution from the coating. High-stability FP cavities are typically made from ultralow expansion (ULE) glass to reduce cavity length changes due to temperature drift around room temperature. Cavity lengths are often 10–20 cm. Under such conditions, the lowest thermal noise instability is typically  $3 \times 10^{-16}$  to  $1 \times 10^{-15}$ , roughly consistent with the best experimentally observed instability<sup>12–15</sup>. To reduce thermal noise, the choice of mirror substrate material ( $E$  and  $\phi_{\text{sub}}$ ), beam radius ( $w_0$ ), cavity length ( $L$ ) and cavity temperature ( $T$ ) can be modified. Each modification presents different technical challenges. Our approach was to fabricate a long cavity featuring a larger beam size and alternative mirror material.

Because the thermal expansion of the cavity must be controlled well, we chose ULE glass as the cavity spacer material. However, the value of  $\phi_{\text{sub}}$  for fused-silica mirror substrates<sup>10,13,16</sup> is more than ten times smaller than that for ULE. Consequently, the

substrate thermal noise term shrinks below that of the thin-film reflective coating (equation (1), second term in parentheses), and  $\sigma_{\text{therm}}$  is reduced by 1.8. Now dominated by the thin-film coating,  $\sigma_{\text{therm}}$  can be further reduced by exploiting its  $1/w_0$  (refs 11, 17) and  $1/L$  dependencies. We therefore chose a long cavity ( $L = 29$  cm) with a longer radius of curvature ( $R = 1$  m) for both cavity mirrors. With these cavity parameters, we reduced the thermal-noise-limited fractional frequency instability to  $1.4 \times 10^{-16}$ .

We constructed two similar cavity systems (Fig. 1) and measured the laser coherence properties between them (see Methods). The frequency noise spectrum of one cavity-stabilized laser is shown in Fig. 2a. The noise spectrum approaches the projected thermal noise for Fourier frequencies around 1 Hz; at higher frequencies, the spectrum is approximately white, with several spikes attributed to seismic noise on one of the cavities. In Fig. 2b, we show the fractional frequency instability, together with  $\sigma_{\text{therm}}$ . During typical best performance, for averaging times below 10 s we observe an instability as low as  $2 \times 10^{-16}$ . Less ideal data sets give a measure closer to  $3 \times 10^{-16}$ . For averaging times  $>10$  s, laser instability typically increases. The measured laser power spectrum is shown in Fig. 2c, with a linewidth of 250 mHz. To minimize thermal drift of the cavity resonance, we engineered the cavity coefficient of thermal expansion (CTE) to cross zero near room temperature (Fig. 2d; see Methods).

With the performance shown in Fig. 2, the cavity-stabilized laser serves well as a low-noise LO to probe the narrow clock transition of an optical-frequency standard, in this case the  $^1\text{S}_0$ – $^3\text{P}_0$  transition of neutral  $^{171}\text{Yb}$  confined in an optical lattice<sup>8</sup>. The first benefit of the low-noise LO is its ability to coherently excite the clock transition for long times (allowing narrower  $\delta\nu$ ). By probing the transition for 0.9 s and stepping the LO frequency by 0.25 Hz every

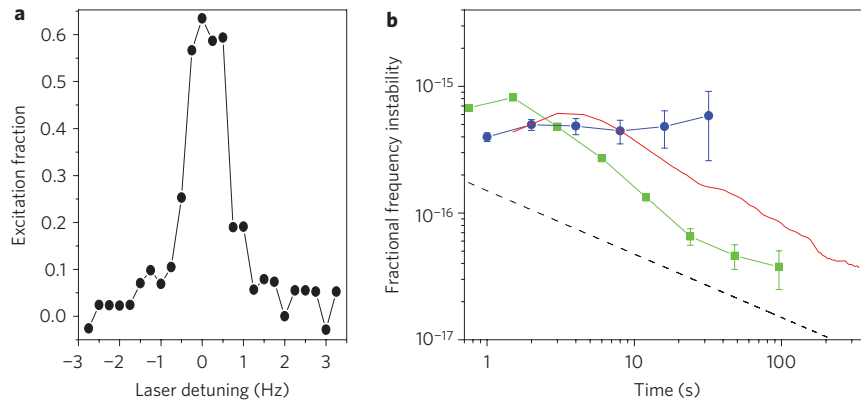


**Figure 3 | Optical clock performance.** **a**, Optical clock transition spectrum of neutral ytterbium atoms. The LO frequency is stepped by 0.25 Hz every cycle, with a probe time of 0.9 s, resolving a spectral linewidth of 1 Hz, FWHM (no averaging). **b**, Instability evaluation of the ytterbium clock using atomic transition. Blue circles are taken from using atomic excitation as an (out-of-loop) frequency discriminator for measuring the LO frequency. Green squares give the in-loop stability (from error signal) when the LO is locked to the atomic transition. The Dick-effect-limited instability (black dashed line) is  $1.5 \times 10^{-16}/\sqrt{\tau}$ . The red curve indicates the stability for interleaved measurements used to assess systematic shifts. One sigma error bars are shown.

experimental cycle, we resolved 1 Hz linewidth (full-width at half-maximum, FWHM) atomic spectra as in Fig. 3a. With a transition frequency of 518 THz, this corresponds to a line quality factor of  $\nu_0/\delta\nu > 5 \times 10^{14}$ , the highest achieved for any form of coherent spectroscopy<sup>18,19</sup>. Combined with a good measurement signal-to-noise ratio, this makes it possible to achieve very low lock instability.

To rigorously assess clock instability (consisting of the LO stabilized to the ytterbium transition), it must be compared to another standard with even lower instability. Anticipating previously unobserved stability levels with this individual system, we instead evaluated the noise levels that determined the clock instability. Although the 0.9 s probe time enables very narrow atomic spectra, it leaves the atomic transition lock sensitive to short-time laser frequency excursions, which occasionally exceed the  $\sim 1$  Hz locking range. For this reason, we chose to operate the system with a 0.3 s probe time ( $\delta\nu \approx 3$  Hz), 40% of the 0.75 s total cycle. Under these conditions and with the LO frequency noise spectrum from Fig. 2a, we calculated the Dick limit to be  $1.5 \times 10^{-16}/\sqrt{\tau}$  (Fig. 3b, dashed line), an order of magnitude of improvement over our previous LO<sup>20</sup>. We tuned the LO frequency on-resonance with the atomic transition and used the measured excitation as a frequency discriminator. This out-of-loop measurement is sensitive not only to LO frequency instability, but also to the noise terms that set the mid-to-long-term instability of the optical standard (including the Dick effect and detection noise of the atom system, such as photon shot noise, quantum projection noise and technical noise). The results of this measurement are shown in Fig. 3b as blue circles, indicating that the optical clock system supports an instability of  $\lesssim 5 \times 10^{-16}$  after just one measurement cycle (see Methods). When we close the loop to lock the LO to the atomic transition, the instability can begin averaging down, as suggested by Fig. 3b (green squares). This is the in-loop error signal stability of the LO lock to the atomic transition, and gives a lower limit to the expected clock instability. At 1 s, we see that our aggressive choice of feedback gain degrades the LO stability. However, by 2 s we begin averaging down, faster than  $1/\sqrt{\tau}$ , so that after 20 s of closed-loop operation, we can reach the anticipated  $(5 \times 10^{-16})/\sqrt{\tau}$  indicated by the out-of-loop signal. Construction of a second ytterbium optical lattice clock, currently under way, will enable even more direct measure of the improved stability. Here, we emphasize a key point: by sufficiently reducing the Dick effect, we have more fully enabled the benefits afforded by the signal-to-noise ratio of a large atom ensemble to achieve this unprecedented level of stability.

This stability enables high-precision frequency measurements at faster speeds than ever before, including characterization of systematic shifts of the ytterbium clock transition<sup>8</sup>. Several important systematic shifts can be studied by interleaving the clock operation between two conditions and looking for a frequency shift. The red trace in Fig. 3b shows the stability of such a measurement, enabling precision at  $< 8 \times 10^{-17}$  at 100 s and averaging down as  $1/\sqrt{\tau}$ . Note that this observed instability is consistent with  $(5 \times 10^{-16})/\sqrt{\tau}$  for normal single operation, accounting for the quadrature sum of uncorrelated noise between the two-setting-interleaved clock operation, as well as the extra cycle time required for dual operation.

However, these powerful optical standards offer still more untapped potential. The Dick limit must be lowered by yet another order of magnitude to reach possible quantum projection noise limits. Efforts to reduce the preparation time in the experimental cycle will help significantly<sup>21</sup>, as will interrogation optimization<sup>4,5</sup>. The effect will continue to get smaller as the LO is further improved, including further reduction of the cavity thermal noise. Many worthwhile efforts can be made here, focusing on one or more of the critical cavity parameters described above, such as increasing the beam size on the mirror (including higher-order cavity excitation<sup>16</sup>) or cryogenic cavity cooling<sup>10</sup>. To make the cavity effectively longer, a multiple-mirror cavity could be used where all but the first and last are folding mirrors. Each mirror introduces uncorrelated thermal noise, so a cavity with  $N$  mirrors and optical length  $L$  between each mirror can have fractional thermal noise scaling as  $\sqrt{2N-3}/[(N-1)L]$  (also enabling a larger average beam size). For our  $L = 29$  cm cavity, with six fused-silica mirrors, the thermal noise instability limit is reduced to  $7 \times 10^{-17}$ .

## Methods

**Laser coherence measurements.** Several milliwatts of laser light at 578 nm (ref. 8) were divided into multiple paths, one to each of the two cavities and one to the ytterbium optical lattice apparatus (Fig. 1). Each cavity was enclosed in a vacuum chamber, which was single-stage temperature controlled (fluctuations over 24 h at a few millikelvin). One important cavity design consideration was the reduction of length changes due to acceleration-induced deformation. We implemented a cavity mounting design, similar to those described in refs 13 and 22, with the cavity resting on four symmetrically placed Viton hemispheres. By doing so, we were able to measure acceleration sensitivity (along gravity) as low as  $1 \times 10^{-11}/(\text{m s}^{-2})$ . The vacuum chamber and optics coupling light to the cavity sat on vibration isolators (one cavity on an active system, the other passive). Each system was located in different parts of the laboratory in independently closed acoustic-shielded chambers. Optical links between the isolated systems and the laser source were made with optical fibre using active phase stabilization<sup>23</sup>. Free-space optical paths were

generally in closed boxes to reduce air currents. The free-running 578 nm laser light was locked to Cavity A using Pound–Drever–Hall (PDH) stabilization, using fast electronic feedback to an acousto-optic modulator (AOM) common to all optical paths, and slow electronic feedback to a piezo-electric transducer on the laser source. Thus, light incident on both cavities was phase-stabilized to Cavity A. To measure the laser frequency noise spectrum, an additional AOM was used to tune laser light incident on Cavity B into resonance, and the PDH signal of Cavity B served as a frequency discriminator. To measure laser frequency stability, the PDH signal from Cavity B was filtered and fed to an AOM to lock the laser frequency of the second beam to the resonance of this cavity. This AOM frequency thus provided the difference between the two cavities, and was counted to determine the frequency stability. The stability shown in Fig. 2 used counting data from an Agilent 53132 and a Stanford SR620. Measurements made using a Pendulum CNT-91 (gate time, 1 s) gave similar measures of stability.

**Cavity thermal expansion properties.** As described in the main text, each cavity consisted of a ULE spacer with fused-silica mirror substrates. Because fused-silica mirrors have a much larger CTE ( $+500 \text{ ppb K}^{-1}$ ) than the ULE spacer ( $\pm 30 \text{ ppb K}^{-1}$ ) to which they are contacted, temperature changes create stress, which bends the mirror substrate and introduces a larger CTE for the composite cavity ( $\text{CTE}_{\text{cav}}$ ) than for ULE alone. To compensate this effect and achieve a very small  $\text{CTE}_{\text{cav}}$ , we took advantage of the CTE dependence of ULE on  $\text{TiO}_2$  doping level and temperature<sup>24</sup>. By obtaining a ULE piece with doping levels corresponding to a room-temperature CTE of  $-40 \text{ ppb K}^{-1}$ , we were able to tune Cavity A temperature so that, combined with the mirror-bending effect, we observed a  $\text{CTE}_{\text{cav}}$  zero crossing at  $32.2(0.1)^\circ\text{C}$  (Fig. 2d). At this temperature (conveniently just above room temperature),  $\text{CTE}_{\text{cav}} < 0.2 \text{ ppb K}^{-1}$  and the thermally driven drifts were minimized. For Cavity B, we located a piece of ULE with small, negative CTE at room temperature and, following the procedure of ref. 25, contacted ULE rings to the back side of the fused-silica mirrors. These rings largely prevent mirror bending from CTE mismatch with the spacer. We again observed a  $\text{CTE}_{\text{cav}}$  zero crossing, this time at  $31.1(0.1)^\circ\text{C}$  (Fig. 2d). After characterizing  $\text{CTE}_{\text{cav}}$  for each cavity, to reduce radiative heat transfer, which at first heats only the mirrors (small thermal mass), we installed radiative heat shields (low-emissivity, polished aluminium) between the temperature-stabilized vacuum chambers and each FP cavity.

**Ytterbium optical lattice apparatus.** The ytterbium optical lattice system consisted of  $\sim 1 \times 10^4$   $^{171}\text{Yb}$  atoms cooled to a temperature of  $10 \mu\text{K}$  and trapped in a one-dimensional optical lattice<sup>8</sup> operating at the magic wavelength where the differential Stark shift on the transition is zero<sup>26,27</sup>. The optical lattice facilitated long interrogation of ultracold ytterbium while eliminating most Doppler and recoil effects. Excitation of the clock transition was detected by monitoring the ground- and excited-state populations after spectroscopic probing to determine the normalized excitation. The measurements recorded in Fig. 3b were from excitation of the  $\pi$ -transition of the  $m_F = 1/2$  state. Owing to first-order Zeeman sensitivity, a magnetic field stability of 0.01% is required over several hundred seconds. This requirement is greatly relaxed when interrogating both  $m_F = \pm 1/2$  states.

In addition to the probe time exciting the transition, the experimental cycle typically included 450 ms dedicated to collecting, cooling and loading atoms into the optical lattice, as well as state preparation and readout. The additional noise processes that presently affect the ytterbium clock instability (at  $\tau = \text{one cycle}$ ) include atom detection noise (quantum projection noise and technical noise) measured at  $\sim 1 \times 10^{-16}$ , and uncompensated optical path phase noise on the ytterbium apparatus measured at  $\leq 2 \times 10^{-16}$ .

Received 23 September 2010; accepted 6 December 2010;  
published online 23 January 2011

## References

- Udem, T. *et al.* Absolute frequency measurements of the  $\text{Hg}^+$  and Ca optical clock transitions with a femtosecond laser. *Phys. Rev. Lett.* **86**, 4996–4999 (2001).
- Chou, C. W., Hume, D. B., Koelemeij, J. C. J., Wineland, D. J. & Rosenband, T. Frequency comparison of two high-accuracy  $\text{Al}^+$  optical clocks. *Phys. Rev. Lett.* **104**, 070802 (2010).
- Bize, S. *et al.* Advances in atomic fountains. *Compt. Rend. Phys.* **5**, 829–843 (2004).
- Dick, G. J. Local oscillator induced instabilities in trapped ion frequency standards. *Proc. Precise Time and Time Interval Meeting* 133–147 (1987).
- Santarelli, G. *et al.* Frequency stability degradation of an oscillator slaved to a periodically interrogated atomic resonator. *IEEE Trans. Ultra. Ferro. Freq. Cont.* **45**, 887–894 (1998).
- Itano, W. M. *et al.* Quantum projection noise—population fluctuations in 2-level systems. *Phys. Rev. A* **47**, 3554–3570 (1993).

- Ludlow, A. D. *et al.* Sr lattice clock at  $1 \times 10^{-16}$  fractional uncertainty by remote optical evaluation with a Ca clock. *Science* **319**, 1805–1808 (2008).
- Lemke, N. D. *et al.* Spin-1/2 optical lattice clock. *Phys. Rev. Lett.* **103**, 063001 (2009).
- Swallows, M. D. *et al.* Precision measurement of fermionic collisions using an  $^{87}\text{Sr}$  optical lattice clock with  $1 \times 10^{-16}$  inaccuracy. *IEEE Trans. Ultra. Ferro. Freq. Cont.* **57**, 574–582 (2010).
- Numata, K., Kemery, A. & Camp, J. Thermal-noise limit in the frequency stabilization of lasers with rigid cavities. *Phys. Rev. Lett.* **93**, 250602 (2004).
- Nakagawa, N., Gretarsson, A., Gustafson, E. & Fejer, M. Thermal noise in half-infinite mirrors with nonuniform loss: a slab of excess loss in a half-infinite mirror. *Phys. Rev. D* **65**, 102001 (2002).
- Young, B., Cruz, F., Itano, W. & Bergquist, J. Visible lasers with subhertz linewidths. *Phys. Rev. Lett.* **82**, 3799–3802 (1999).
- Millo, J. *et al.* Ultrastable lasers based on vibration insensitive cavities. *Phys. Rev. A* **79**, 053829 (2009).
- Ludlow, A. D. *et al.* Compact, thermal-noise-limited optical cavity for diode laser stabilization at  $1 \times 10^{-15}$ . *Opt. Lett.* **32**, 641–643 (2007).
- Webster, S., Oxborrow, M. & Gill, P. Subhertz-linewidth Nd:YAG laser. *Opt. Lett.* **29**, 1497–1499 (2004).
- Notcutt, M. *et al.* Contribution of thermal noise to frequency stability of rigid optical cavity via Hertz-linewidth lasers. *Phys. Rev. A* **73**, 031804 (2006).
- Levin, Y. Internal thermal noise in the LIGO test masses: a direct approach. *Phys. Rev. D* **57**, 659–663 (1998).
- Chou, C. W. *et al.* Optical clocks and relativity. *Science* **329**, 1630–1633 (2010).
- Boyd, M. M. *et al.* Optical atomic coherence at the 1-second time scale. *Science* **314**, 1430–1433 (2006).
- Oates, C. W. *et al.* Stable laser system for probing the clock transition at 578 nm in neutral ytterbium, in *Proc. 2007 IEEE Int. Freq. Cont. Symp.* 1274–1277 (IEEE, 2007).
- Westergaard, P. G., Lodewyck, J. & Lemoine, P. Minimizing the Dick effect in an optical lattice clock. *IEEE Trans. Ultra. Ferro. Freq. Cont.* **57**, 623–628 (2010).
- Webster, S. A., Oxborrow, M. & Gill, P. Vibration insensitive optical cavity. *Phys. Rev. A* **75**, 011801 (2007).
- Ma, L. S., Jungner, P., Ye, J. & Hall, J. L. Delivering the same optical-frequency at 2 places — accurate cancellation of phase noise introduced by an optical-fiber or other time-varying path. *Opt. Lett.* **19**, 1777–1779 (1994).
- Fox, R. W. Temperature analysis of low-expansion Fabry–Perot cavities. *Opt. Express* **17**, 15023–15031 (2009).
- Legero, T., Kessler, T. & Sterr, U. Tuning the thermal expansion properties of optical reference cavities with fused silica mirrors. *J. Opt. Soc. Am. B* **27**, 914–919 (2010).
- Ye, J., Kimble, H. J. & Katori, H. Quantum state engineering and precision metrology using state-insensitive light traps. *Science* **320**, 1734–1738 (2008).
- Katori, H., Takamoto, M., Pal'chikov, V. G. & Ovsiannikov, V. D. Ultrastable optical clock with neutral atoms in an engineered light shift trap. *Phys. Rev. Lett.* **91**, 173005 (2003).
- Dawkins, S. T., McFerran, J. J. & Luiten, A. N. Considerations on the measurement of the stability of oscillators with frequency counters. *IEEE Trans. Ultra. Ferro. Freq. Cont.* **54**, 918–925 (2007).

## Acknowledgements

The authors acknowledge support regarding optical frequency comb measurements from S. Diddams, T. Fortier and M. Kirchner, optical cavity measurement and equipment loan from J. Bergquist, T. Rosenband and C. Chou, and useful discussions with J. Bergquist and G. Santarelli. The authors also thank L. Hollberg for design guidance and useful discussions. Y.Y.J. and L.S.M. acknowledge support from the National Basic Research Program of China (grant no. 2010CB922903) and the Science and Technology Commission of Shanghai Municipality (grant no. 07JC14019).

## Author contributions

Y.Y.J., A.D.L., N.D.L., and J.A.S. carried out the laser frequency or optical clock measurements reported here. Y.Y.J. designed and constructed many aspects of the stable cavity system and made many of the laser frequency measurements. R.W.F. carried out thermal design simulations and measurements. A.D.L. and N.D.L. designed and constructed many aspects of the stable cavity system. A.D.L., L.S.M., and C.W.O. supervised this work. All authors contributed to the final manuscript.

## Additional information

The authors declare no competing financial interests. Reprints and permission information is available online at <http://npg.nature.com/reprintsandpermissions/>. Correspondence and requests for materials should be addressed to A.D.L.